NASA Glenn Propulsion Systems Lab: 2012 Inaugural Ice Crystal Cloud Calibration Procedure and Results

Judith F. Van Zante [1]
NASA Glenn Research Center, Cleveland, OH 44135

and

Bryan M. Rosine [2]
Jacobs Engineering, Cleveland, OH 44135

The inaugural calibration of the ice crystal and supercooled liquid water clouds generated in NASA Glenn's engine altitude test facility, the Propulsion Systems Lab (PSL) is reported herein. This calibration was in support of the inaugural engine ice crystal validation test. During the Fall of 2012 calibration effort, cloud uniformity was documented via an icing grid, laser sheet and cloud tomography. Water content was measured via multi-wire and robust probes, and particle sizes were measured with a Cloud Droplet Probe and Cloud Imaging Probe. The environmental conditions ranged from 5,000 to 35,000 ft, Mach 0.15 to 0.55, temperature from +50 to -35 F and relative humidities from less than 1% to75% in the plenum.

Nomenclature

CDP	=	Cloud Droplet Probe, drop sizer, 2-50 um
CIP	=	Cloud Imaging Probe Grayscale, drop sizer, 15-930 um
DeltaP	=	Pwat - Pair (psid)
GPM	=	gallons per minute (water flow rate)
IRT	=	Icing Research Tunnel
LWC	=	Liquid Water Content (g/m3)
MVD	=	Median Volumetric Diameter (um)
MW	=	Multi-wire, water content sensor
Pair	=	spray nozzle atomizing air pressure (psig)
PSL	=	Propulsion Systems Laboratory
Pwat	=	spray nozzle water pressure (psig)
RH	=	Relative Humidity
RP	=	Robust Probe
S####	=	Calibration test spray condition (4-digit number)
SBCA	=	spray bar cooling air
STA 1	=	calibration plane in the 36-in duct
TWC	=	Total Water Content (g/m3)
um	=	micron

[1] Icing Technnical Lead, Facilities and Test Division, NASA Glenn Research Center, and AIAA Senior Member.
[2] Electrical Test Engineer, Jacobs Engineering, Inc, Facilities and Test Division, NASA Glenn Research Center.

I. Introduction

NASA Glenn Research Center's Propulsion Systems Laboratory, PSL, Test Cell #3 is an engine altitude test stand that is now capable of producing an icing cloud. In 2010, American Recovery and Reinvestment Act (ARRA) stimulus funding was allocated for the necessary facility modifications to generate ice crystals. This major undertaking was in response to the recently diagnosed threat of engine ice crystal icing. High ice water content clouds can cause power loss events in all class of turbine engines[1]. These power loss events include roll back, flame out, stall, surge, and foreign object damage. The regulatory agencies are moving to require that engine manufacturers certify turbine engines in this high ice crystal environment[2]. Figure 1 depicts the altitude and temperature regions of concern for the FAA FAR 33 Appendix D ice crystal threat, PSL's capabilities and the primary focus region of this inaugural calibration.

This paper reports on the inaugural cloud characterization effort conducted to support the inaugural engine ice crystal icing validation test. For the validation test, the same the highly instrumented engine that previously had been flown in a high ice crystal environment was installed in PSL.[3] On board sensors recorded the cloud conditions when the engine rolled back during the flight campaign. These flight and atmospheric conditions were recreated in PSL, and the engine rolled back in a similar fashion.[4]

II. Facility Description

A. Basic PSL Facility

PSL Test Cell #3 is an altitude chamber that can run a turbine engine and deliver an ice crystal or supercooled liquid cloud. With the icing system installed, PSL-3 can run over a significant portion, but not all, of its full operating range. With the icing system installed, the facility can pump its chamber down to 2.5 psi, the equivalent of 41,000 ft, run upto Mach 0.8, deliver a mass flow rate upto 330 lbm/s, and control the total air temperature between +50 to -60 F. Most engine, clipped fan or driven rig tests are direct connect. Briefly described herein are the facility elements required for cloud generation, a full facility description can be found in Ref. 5.

Externally compressed, conditioned air is supplied through a 5.5-ft duct called Plane 56. Steam for humidity control is injected here. As can be seen from the facility overview in Fig. 2, the steam-enriched airflow then enters a circular 18-ft diameter plenum, flows through a flow straightening screen then the spray bars. A fiberglass contraction section necks the flow down to an 86-in diameter. Downstream of this, the subsequent ducting is configurable for different testing needs. For this calibration effort, the final duct diameter was 36-in. The calibration plane, STA 1, was approximately 44-ft downstream of the spray bars. The overall contraction ratio was 27:1. The 36-in duct continued another 2-ft before becoming a free jet that exhausted into the chamber. A much more complete description of the PSL facility and new icing system can be found in Ref. 5.

B. Icing System

The spray bar system was designed by Cox and Co., under contract. It consists of 10 horizontal spay bars that mostly span the width of the plenum, as shown in Fig. 3a. A feature unique to PSL spraybars is the spray bar cooling air or SBCA. As can be seen if Fig. 3b, eight 8 cooling air ports surround each nozzle. These were added to aide the cooling and freeze-out of the liquid water drops. The SBCA is an optional system. If needed, it can deliver air chilled to -40F at upto 30 psig. These small jets also have the effect of breaking up the water stream, thereby making smaller drops.

Each bar contains the same internally mixed nozzle design as NASA Glenn's sister icing facility, the Icing Research Tunnel, IRT. These are the Standard and Mod1 nozzle sets; a Standard nozzle flows almost three times more water than a Mod1 nozzle. The bars are fed with one water line and two air lines, one to the Standards, and one to the Mod1s. Unlike the IRT, the nozzle location is fixed. As can be seen in Fig. 4, the Standard and Mod1 nozzles alternate.

The spray bar operator controls the atomizing air pressure, Pair, from 10 to 100 psig. The water pressure, Pwat, in the 10 spray bars are controlled with three manifolds: one each for bars 1-3, 4-7 and 8-10. The operator controls the Pwat, so that the DeltaP = Pwat - Pair is between 5 and 150 psid. All spray bar pressures are gage, relative to the pressure altitude set. The maximum water flow rate is 10 GPM. An operator also controls the temperatures of the atomizing air and water. For an ice crystal cloud, these are set to nominally 45 F, as cold as possible so the nozzles do not freeze; for a supercooled liquid cloud, the nozzles are run as in the IRT, nominally at 180 F. It is possible to set intermediate temperatures, but this effect has not yet fully been explored.

III. Calibration Procedure and Results

The cloud characterization was conducted at a primary target environmental condition, and spot checked at a secondary environmental condition. The primary condition is "high altitude, cruise Mach and tropical day temperature"; the secondary condition is similarly "higher altitude, cruise Mach and tropical day temperature". Since the secondary altitude is higher, the actual temperature is colder. Both these two points are contained within the Calibration Region circle noted in Fig. 1. The target relative humidity, RH, in the plenum was 50%, the maximum allowed so as to not condense on the flow straightening screens. It can be assumed that the relative humidity was higher at STA 1, but this was not successfully measured. A few parameter sweeps were conducted around these target conditions. During the characterization effort, the altitude ranged from 5 to 35 kft, the temperature from 55 to -35 F, and the Mach from 0.15 to 0.55. The RH varied from <1 to 75%. Exploring RH will be showcased in the paper.

The ice crystal cloud targets for this calibration effort were LWC = 0.5 to 9 g/m^3 and MVD = 40 to 60 um. However, the calibration also explored the largest MVD possible. The icing cloud was characterized at a given environmental condition by setting a Pair, and increasing DeltaP in a systematic fashion. The same conditions were run for each of the four probes mounted at the center of the STA 1 duct to measure the total or liquid water content, TWC or LWC, and particle size reported as median volumetric diameter, MVD. These measurements occurred after diagnosing the cloud uniformity.

A. Cloud Uniformity

The first step was to establish the nozzle patterns so that the cloud (1) did not impact the plenum or contraction walls, and (2) was as uniform as possible. Cloud uniformity was documented at STA 1 via three methods, one accretion-based and two optical. With the goal of this test focused on larger particles and higher TWCs, exploring the Mod1 nozzles was quickly abandoned due the the compressed time available. The Standard nozzles were run in either a “full” or a “half” mode. That is, within the circle of nozzles that did not hit the plenum, either every Standard was turned on, “Full”, or every other, “Half”. Details of the Half nozzle pattern are shown in Fig 4.

1. Accretion-based

For the accretion-based method, supercooled liquid water accreted on a 3x6-in mesh grid with 0.125-in wide rectangular bars, shown in Fig. 5a. The ice thickness can be used to calculate the LWC as long as the accreted ice does not significantly change the collection efficiency of the bare grid. Therefore, the air temperature must be cold enough so that the freezing fraction is near or greater than 1.0, and the spray time must be fairly short, 15 to 300 sec, depending on LWC. The local LWC can then be calculated as described in Eq. 1 from the ice thickness measurement at each measurement point:

$$LWC = C * d / (V * t * Eb) \quad (1)$$

where d = ice thickness (in), V = airspeed (knots), t = spray time (sec), Eb = collection efficiency, and C = 43440, which includes unit conversion coefficients and an ice density value of 0.88 g/m3. More details on the grid uniformity method can be found in Ref. 6.

To measure the ice thickness automatically and remotely, there was an attempt to deposit a thin layer of talcum powder on the ice then measure thickness via 12 laser proximity probes. This approach worked reasonably well for a

few sprays, see Fig. 5b, but ultimately had to be abandoned as the powder did not alway deposit on the grid with sufficient uniformity. The alternate method was to physically measure the ice thickness at the center of each vertical element with calipers. This approach required that the chamber be repressurized (about 30 min), then opened to the ambient environment (thereby eliminating any temperature control) after which a technician and engineer entered the chamber to make the measurements. Fate would place this night of testing during a heat wave, and the ice became too soft to measure after about 20 min. Even so, this method was able to provide reasonable validation for the primary diagnostic, the laser sheet. A comparison of the caliper measurement and a cross-section from the laser sheet data across the horizontal center of the duct is shown in Fig. 5c.

2. Optical

The other two methods, laser sheet and tomography, were optical, and could be used with either liquid or solid particles at any airspeed or temperature. Both these methods are extremely efficient – 70 sprays in a run shift vs 7 with the grid – and are described more fully in Ref. 7. The primary diagnostic for the initial calibration was the laser sheet and CCD camera. As can be seen in Fig. 6a and b, a laser beam was expanded to 24-in, and passed just downstream of the duct exit. A CCD camera measured the light intensity scattered as the cloud particles passed through the sheet. Knowing the mean particle size distribution provided an anchor for calculating particle number density and hence TWC. A sample intensity plot (counts/1000) is shown in Fig. 6c.

The light extinction tomography system, for this test, was installed aft of the Calibration Duct exit for the last two test runs. In the tomography plane, 60 lasers issue light sequentially that was recorded by each of the 120 detectors, see Fig. 7a. Sheet generating optics were placed at each laser diode so that its light flared to 300 deg, and could be seen by all but the several adjacent detectors, as depicted in Fig. 7b. An algorithm based upon the light extinction provided the cloud uniformity over the full duct at significantly higher resolution than the grid. Once the cloud was sampled and averaged; it took about 3-s to process and display the image. A sample intensity (a. u.) surface area plot is shown in Fig. 7c.

The plan is that this tomography duct will be permantely installed in PSL. It is very sensitive, and can detect spray bar failures, such as a frozen-open leaky nozzle during a spray off condition, or frozen-shut nozzles during a "fire hose" full nozzle pattern spray.

Sample tomography uniformities at the primary condition are shown in Fig. 8. A fairly low particle density spray is shown in Fig. 8a, where half the nozzles are spraying in a lower TWC, higher MVD case. A fairly high particle density spray is shown in Fig. 8b with a higher TWC, and lower MVD. The tomography system seems capable over both of these sets of conditions.

B. Total Water Content

1. Single point measurements

The water content was measured at the center of the duct with either a multi-wire, MW, or robust probe, RP, shown mounted in the center of STA 1 in Fig. 9. Both instruments are made by SEA (Mansfield Hollow, CT). The MW has four elements within the the anti-iced probe head. They are a 0.021-in or 0.5-mm wire (Multi021), 0.083-in or 2-mm cylindrical tube (Multi083), and a 2-mm half-pipe (MultiTWC). The wire and cylindrical tube primarily measure LWC while the half pipe captures both LWC and ice particles. The half-pipe therefore measures total water content, TWC. The fourth element is a compensation wire which is placed behind the center element and parallel to the flow. It is designed to stay dry so that it tracks air temperature, air pressure and airspeed effects only. The four heated elements are held at a constant temperature of 140 C. The power required to maintain this temperature is proportional to the amount of water each element must evaporate. SEA defines the LWC and IWC calculations respectively in Eq. 2 and (3)[8]:

$$LWC\left(\frac{g}{m^3}\right) = \frac{C * P_{sense,wet}}{\left[L_{evap} + (T_{evap} - T_{amb})\right] * V * L_{sense} * W_{sense}} \tag{2}$$

and

$$IWC\ \left(\frac{g}{m^3}\right) = \frac{C * P_{sense,wet}}{\left[L_{evap} + C_{liq}\left(T_{evap} - T_{amb}\right) + L_{fus} + C_{ice}\left(T_o - T_{amb}\right)\right] * V * L_{sense} * W_{sense}} \quad (3)$$

where C = 2.389*10^5, $P_{sense,wet} = P_{sense,total} - P_{comp}$ = wet power (W) measured by the sense element, $P_{sense,total}$ is the total power measured by the element, and P_{comp} is the power measured by the compensation element. L_{evap} = latent heat of evaporation (cal/g), C_{liq} = specific heat of vaporization (cal/g/C) = 1.0, T_{evap} = evaporative temperature (C), T_{amb} = ambient static temperature (C), L_{fus} = latent heat of fusion (cal/g), C_{ice} = specific heat of fusion (cal/g/C), T_o = melting temperature (C), L_{sense} and W_{sense} = length and width respectively of the sense element (mm) and V = true airspeed (m/s).

A collection efficiency correction for the half-pipe element was determined and applied for analysis. This collection efficiency, Eb, is a function of airspeed, drop size and geometry. For this design, Eb was calculated by the FWG two-dimensional particle trajectory code.[9]

The half-pipe is the sensor used for TWC measurements, the other two MW elements, however, are useful for indicating percent freeze-out or the percentage of ice crystal to liquid water at the measurement point. Because the wires are heated, they will have a response even in a 100% ice crystal environment[6, 10]. This response is typically less than 10% of the TWC. The fully glaciated condition can be ascertained by a lack of accretion on any unheated surfaces. The MW time trace data shown in Fig. 10 were taken at the primary calibration condition, except while the static air temperature at STA 1, TS1, was cooling down. The spray conditions were held constant and the spray bar air and water temps were cold, 45 F. One can see the percent freeze-out increase with decreasing air temperature. The calculated wet bulb temperature, Twb, is also indicated in deg C.

The RP has a half-pipe element similar to the MW, reinforced with a stainless steel backing but no columating tube or compensation wire. The width of the RP is 3.8-mm, compared to the 2.0-mm width of the half-pipe in the MW. It should be noted that for the RP to operate properly in PSL's harshest cloud conditions, SEA personnel had to modify its PID control loop parameters.

Sample TWC results are shown in Fig. 11. A typical TWC vs. DeltaP trend can be seen in Fig. 11a for one Pair line, Pair = 15 psig. The MVD ranged from 31 to 83 um. Results for both the full and half nozzle patterns are shown. As expected, the TWC nearly doubles for twice the number of nozzles spraying. The importance of controlling RH can be seen in Fig. 11b. An RH sweep from 2 to 75% shows that the TWC increases from 3.91 to 4.17 g/m^3. For this reason to control evaporation, the RH is held constant at 50% in the plenum. Higher RH caused some pressure drop across the upstream flow straightening screens, likely due to ice accretion.

2. Bulk TWC calculations

Calculating bulk TWC is the final step once the intensity from the cloud uniformity and center TWC are known for a given set of conditions. This is done by equating the average of the central 1-in square intensities ($I_{0,0}$ in Eq. 4 below) to the measured TWC from the MW or RP. This TWC/Intensity ratio is then applied to the entire intensity data set. From there, an inner diameter circle can be chosen, typically for this case it was the inner 24" circle. TWC values at each point (pixel) times the area they cover within that circle are summed, then divided by the area within that 24" circle, see Eq. 4.

$$\text{Bulk TWC} = \sum_{i,j}^{n,m} I_{i,j} \times \frac{TWC_{0,0}}{I_{0,0}} \times A_{i,j} \Big/ \sum_{i,j}^{n,m} A_{i,j} \quad (4)$$

where i,j represents the two-dimensional coordinate of each pixel with associated measured intensity, I, and area, A, values. Coordinate (0,0) is centered in the duct, where the TWC measurement is made.

In Fig. 12, intensities from both the laser sheet and tomography duct for the same set of conditions have been converted to TWC values. The TWC measurement came from the RP, Spray 2423: primary condition, Half Standard nozzles, Pair = 20 psig, DeltaP = 40 psid. The water injected was 2.81 GPM. The laser sheet data was obtained for

the same conditions the next day, S2523, and the tomography duct four days later, S2923. For the inner 24-in circle, Table 1 summarizes the bulk and local maximum TWC values calculated from the two optical methods. The ratio is the bulk to measured TWC value. From this and similar cases, the laser sheet and tomography duct show overall good agreement.

Table 1. Comparison of Bulk TWC to Center Measured value for the various methods

	TWC Circle Dia (in)	TWC_RP (g/m^3)	Bulk TWC (g/m^3)	Max TWC (g/m^3)	Bulk / RP ratio (%)
Tomography (S2923)	24	3.30	2.44	3.58	74.0
Laser Sheet (S2523)	24	3.30	2.44	3.74	74.1

C. Drop Sizing

Particles were measured by combining the drop distributions from two probes, the Cloud Droplet Probe (CDP) and Cloud Imaging Probe - Grayscale (CIP). Both instruments, shown installed at STA 1 in Fig. 13 were made by DMT (Boulder, CO).

The CDP measures particles from 2 to 50 um via a forward-scattering technique. Because of this, the CDP was only used in supercooled liquid conditions. The authors are not sure that light scattered through ice crystals yields valid measurements. The CIP, which measures particles 15 – 930 um, on the other hand, utilizes a shadowing technique. It can be used in both supercooled liquid and ice crystal conditions. The grayscale settings vetted the IRT (trigger at 66% shadow) were verified in PSL and used. Both probes are used at a fairly slow airspeed, around 130 kts.

A sample drop size distribution for supercooled liquid water conditions is shown in Fig. 14a. The Number Density plotted is the number of counts in each size bin normalized by the air speed, sample area and bin width. The mean bin diameter is used to calculate the volume in each bin. This is plotted in Fig. 14b. The MVD is the value at the 0.5 mark.

Finally, the MVD sensitivity to plenum RH is shown in Fig. 15. At altitude but warm temperature and slow airspeed, for a given set of spray conditions, one can see that the MVD decreases 25% with increasing RH. This is as expected and points to the importance of controlling relative humidity. The supply air is extremely dry, dew point temperature is -70F. The dry air evaporates moisture from the particles to the point of full evaporation of the smallest drops. The larger drops survive, just get a little smaller. Losing the balance of the smallest drops drives the median volumentric diameter higher.

IV. Conclusion

The inaugural PSL ice crystal calibration was completed in a timely manner with reasonable results. Time and cost constraints disallowed a full exploration of all the parameter space PSL can offer. Rather, the calibration effort focused on the primary and secondary flight conditions for the upcoming engine validation test. These defined the altitude, Mach and air temperature. Another parameter, relative humidity, was explored and typically set to 50% in the plenum; this was to control evaporation and recondensation effects. The ice crystal cloud targets were LWC = 0.5 to 9 g/m^3, MVD = 40 to 60 um. However, the calibration explored the largest MVD possible. At these flight conditions, the cloud particles are fully glaciated upto 100 um, although larger drops can be produced.

The ice crystal and supercooled liquid water clouds were characterized with two hot-wire type TWC probes: the Multi-wire and Robust probe. The particle sizes were characterized by combining the drop size distributions from the CDP and CIP-GS. A crucial element of this calibration was to determine the cloud uniformity so that a bulk TWC could be calculated. Both accretion-based and optical methods were utilized. There was very reasonable agreement between these three methods, with the non-intrusive, optical methods being significantly more efficient.

Acknowledgments

This calibration effort was funded by NASA AEST and ATP programs. The authors wish to acknowledge and thank the superior effort given by the entire PSL team. Mechanical Engineers: Tom Griffin, Dennis Dicki, Queito Thomas, Jack Kowalewski, JP Kirkegaard,. Electrical Engineers: Paul Lizanich, Pam Poljak, Steve Pesek, Bryan Rosine, Morgan Pugh, Vince Anton, Kin Wong. Mechanical Technicians: Jeff Bobonik, John Wargo, Kent Smith, Adam Wasylyshyn, Jim Sexton, Jason Jacko, Chris Yager, Jeff Luptak. Electrical Technicians: Ken Trsek, Joe Switala, Dan Erbacher, Ryan Brown, Jeff Paulin, Mike Garapic, Eric Stevens, John Brodkowski. Engine icing expert from the Icing Branch, Mike Oliver, and the cloud specialists from the Icing Research Tunnel: Bob Ide, Laura Steen.

References

[1] Mason, J.G., Strapp, J.W. and Chow, P., "The Ice Particle Threat to Engines in Flight", 44th Aerospace Sciences Meeting and Exhibit, AIAA, January 9-12, 2006, Reno, NV

[2] FAA FAR 14 CFR Parts 25 and 33, "*Airplane and Engine Certification Requirements in Supercooled Large Drop, Mixed Phase, and Ice Crystal Icing Conditions*", Federal Register / Vol. 75, No. 124 /Tuesday, June 29, 2010 / Proposed Rules, NPRM 10-10.

[3] Goodwin, Ronald,V.and Dischinger, David,G.,"Turbofan Ice Crystal Rollback Investigation and Preparations Leading to Inaugural Ice Crystal Engine Test at NASA PSL-3 Test Facility", 6th Atmospheric and Space Environments Conference, AIAA, Atlanta, GA, June 16-20, 2014 (to be published)

[4] Oliver, Michael J., "Validation Ice Crystal Icing Engine Test in the Propulsion Systems Laboratory at NASA Glenn Research Center", 2014 AIAA Aviation*, AIAA Meeting Papers on Disc* [CD-ROM], to be published.

[5] Griffin, Thomas A., Dicki, Dennis J., Lizanich, Paul J., "PSL Icing Facility Upgrade Overview," 2014 AIAA Aviation*, AIAA Meeting Papers on Disc* [CD-ROM], to be published.

[6] Van Zante, Judith F., Ide, Robert F., Steen, Laura E., "NASA Glenn Icing Research Tunnel: 2012 Cloud Calibration Procedure and Results", *4th AIAA Atmospheric and Space Environments Conference*, New Orleans, *AIAA Meeting Papers on Disc* [CD-ROM], Jun 2012.

[7] Bencic, Timothy J., Fagan, Amy F., Van Zante, Judith F., Kirkegaard, J.P., Rohler, David P., Maniyedath, Arjun, and Izen, Steven H., "Advanced Optical Diagnostics for Ice Crystal Cloud Measurements in the NASA Glenn Propulsion Systems Laboratory", 2013 AIAA Atmospheric and Space Environments Conference*, AIAA Meeting Papers on Disc* [CD-ROM].

[8] Science Engineering Associates, "WCM-2000 Users Guide", http://www.scieng.com/ Oct 6, 2010.

[9] Frost, W., "*Two-Dimensional Particle Trajectory Computer Program*," Interim Report for Contract NAS3–22448, Mar. 1982.

[10] Van Zante, Judith. F., Ide Robert. F, Addy, H. Eugene., "*PSL Technology Demonstration Testing*", to be published as a NASA TM.

Figures

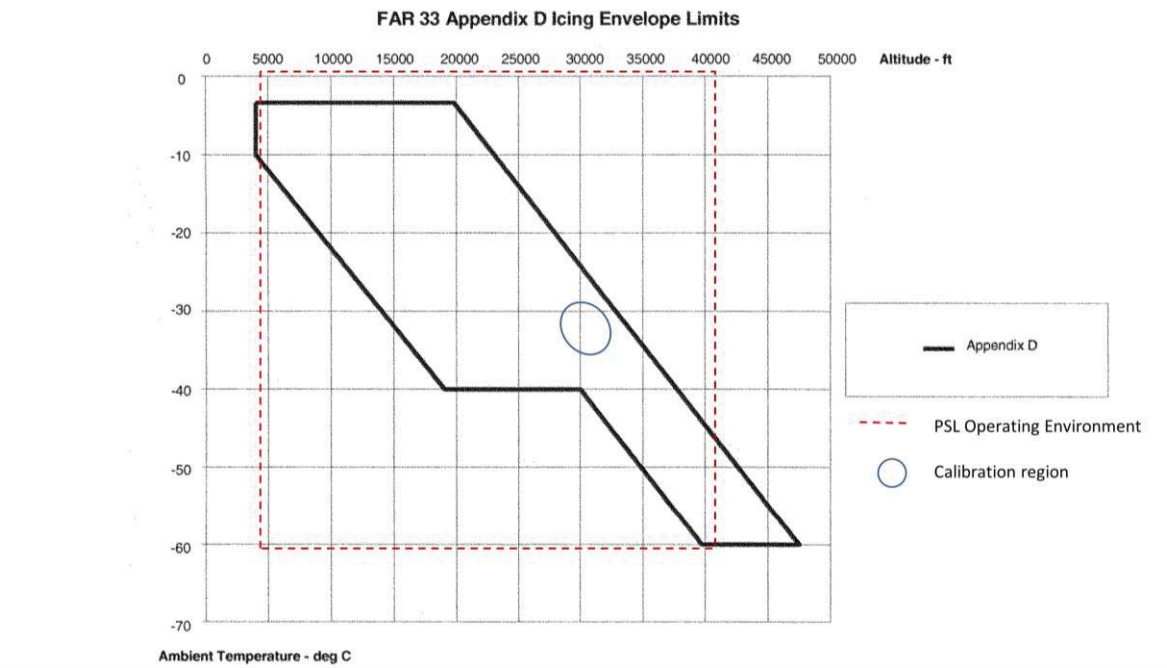

Figure 1. PSL operating environment compared to proposed FAA FAR 33 Appendix D [Ref. 2] (and EASA Appendix P) Convective Cloud Ice Crystal Envelope. The range containing the two environmental conditions at which the cloud characterization occurred are indicated.

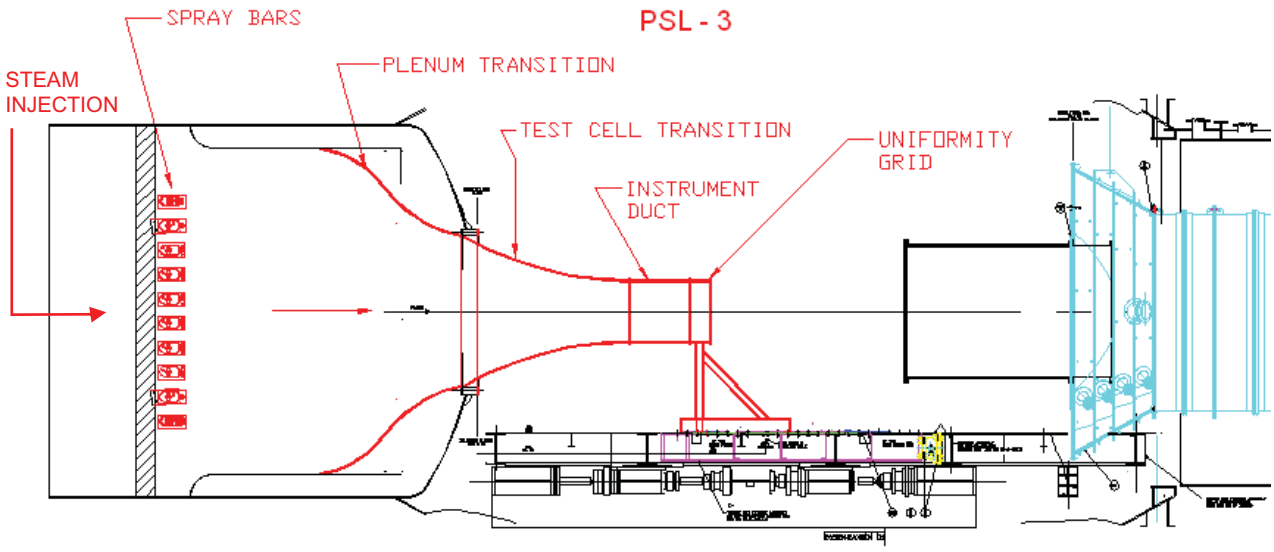

Figure 2. PSL Test Cell #3 facility schematic showing the steam injection upstream of the screen and spraybars in plenum, the transition and 36-in calibration ducts.

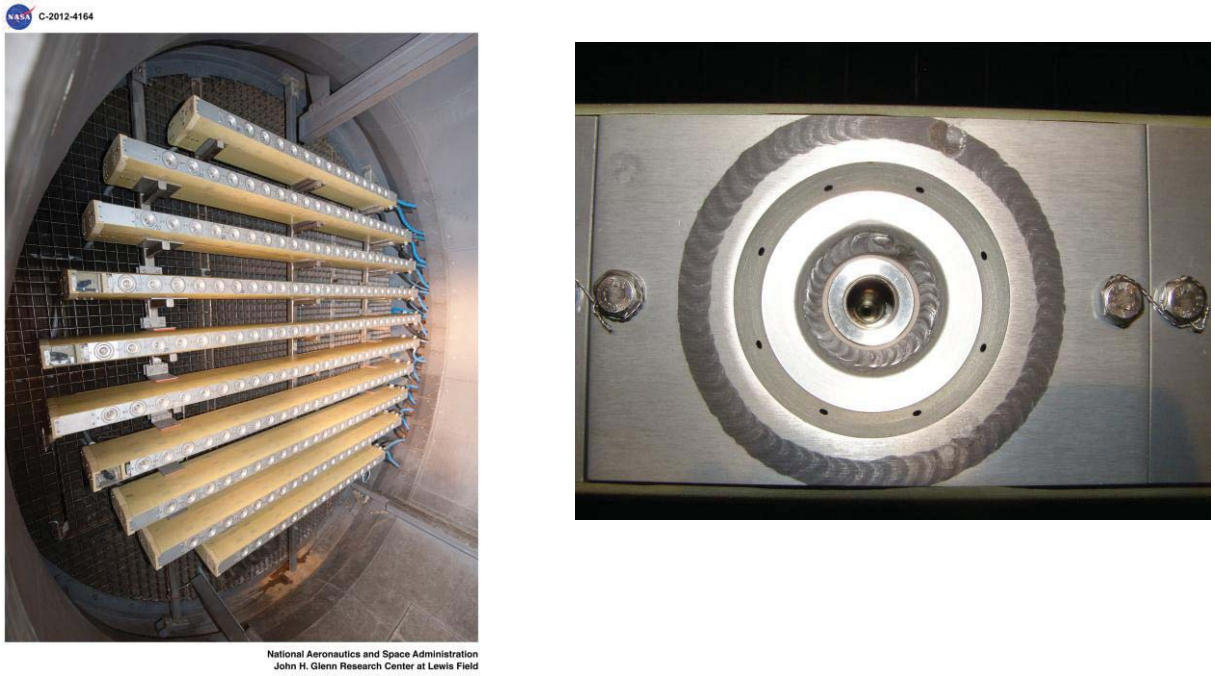

(a) (b)

Figure 3. Spraybar system: (a) all 10 bars installed in the plenum, (b) close-up of a single nozzle; the spray issues from the center nozzle, the optional cooling air issues from the eight surrounding ports.

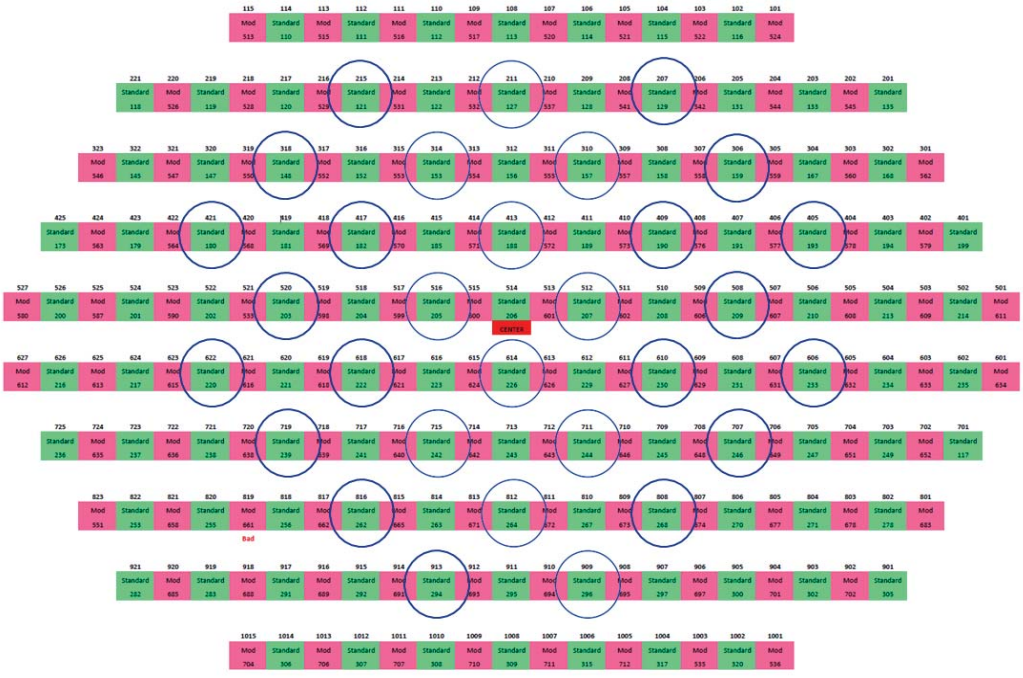

Figure 4. Schematic of the Standard (green) and Mod1 (pink) nozzle locations. Circled in blue are the nozzles in the "half" pattern.

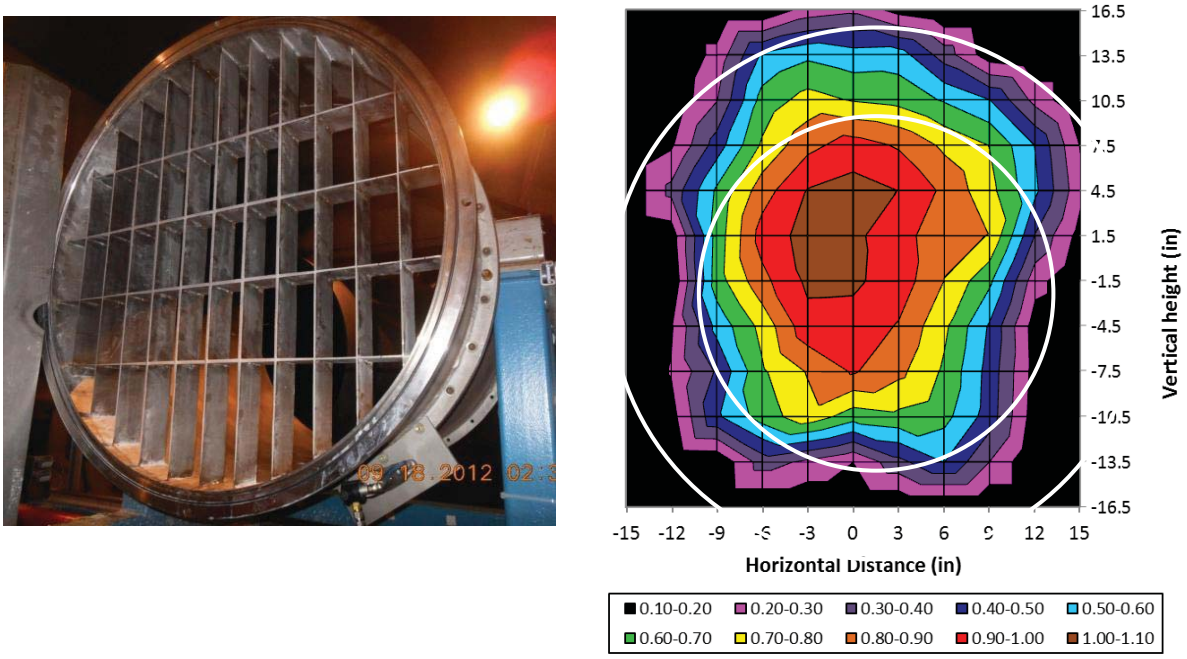

(a) (b)

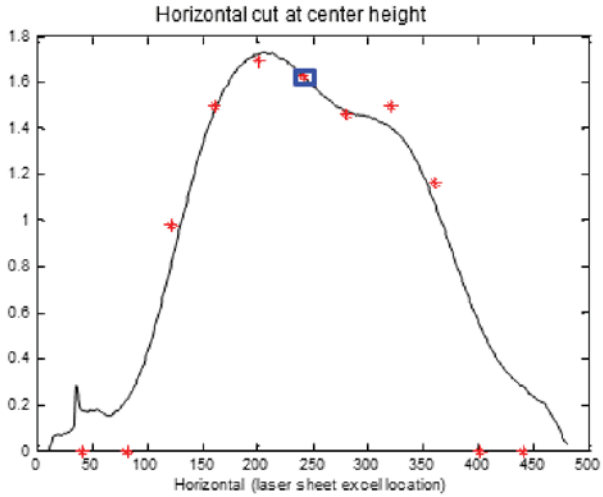

(c)

Figure 5. LWC Uniformity Grid: (a) image of grid, (b) LWC ratio surface area plot for Spray 203, measured by laser proximity probes. LWC values are ratiod to central LWC value. The inscribed circles are 24-in and 36-in. (c) comparison of caliper grid measurement at center height (+) to intensity measurement from laser sheet (line). The blue box indicates the point which anchors the caliper measurement to the intensity value.

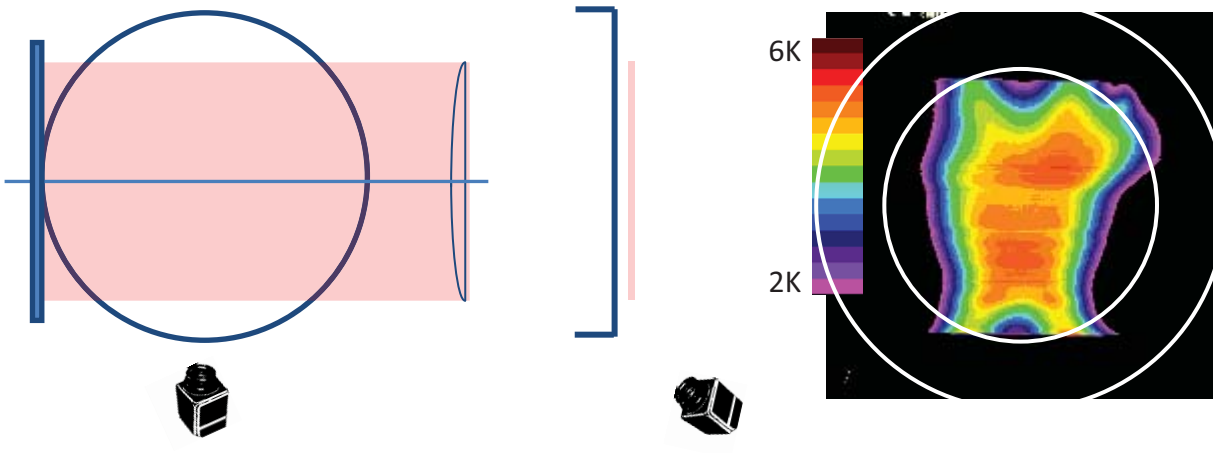

(a) (b) (c)

Figure 6. Laser Sheet Uniformity. Setup schematic of duct, laser sheet and CCD camera: (a) aft looking forward view of the 24-in sheet across the 36-in duct, (b) side view, and (c) sample intensity surface area plot for Spray 2500 with intensity values (counts/1000) indicated; the inscribed circles are 24-in and 36-in.

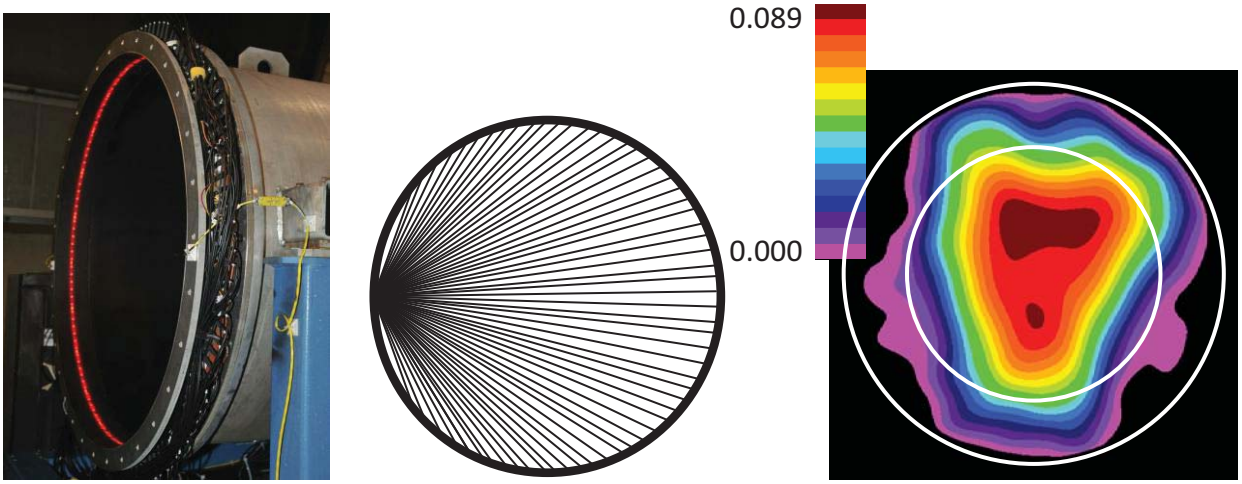

(a) (b) (c)

Figure 7. Tomography Uniformity: (a) all lasers firing in 36-in duct, (b) schematic depicting one laser, expanded 300 deg, hitting all detectors in its beam path, and (c) sample intensity surface area plot for Spray 2923, the same conditions as Spray 2500 in Fig. 4 with intensity values (a. u.) indicated; the inscribed circles are 24-in and 36-in.

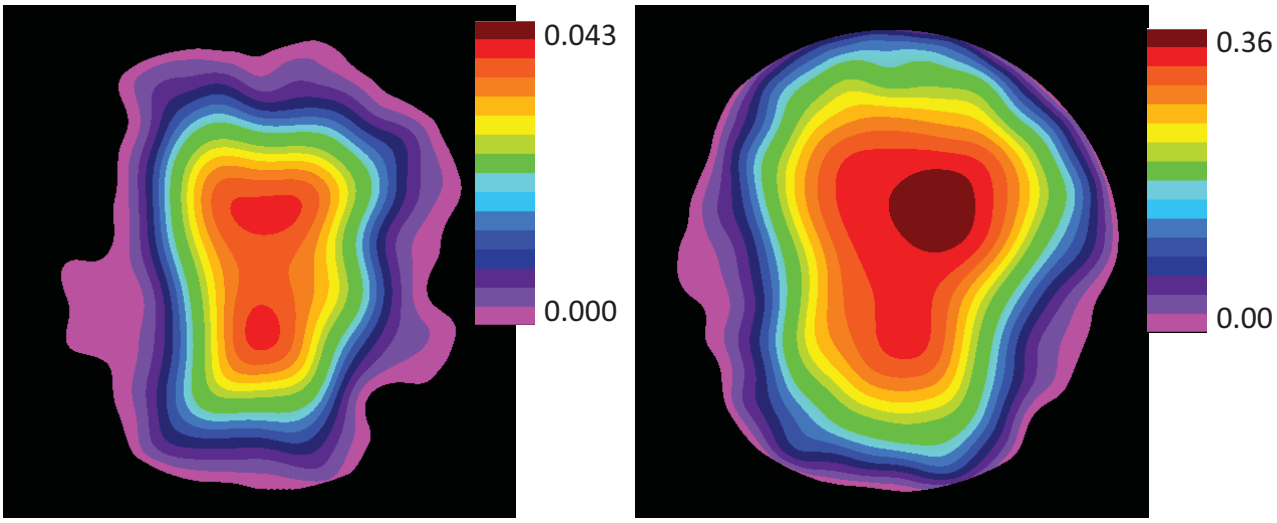

(a) (b)

Figure 8. Sample uniformity results from the tomography intensities at the primary condition. (a) S2963: Half Standard nozzles, Pair = 10 psig, DeltaP = 25 psid, MVD > 100 um, TWC from MW = 2.95 g/m^3, spray injection = 1.80 GPM. (b) S2917: Full Standard nozzles, Pair = 50 psig, DeltaP = 130 psid, MVD = 40 um, TWC from MW = 4.90 g/m^3, spray injection = 8.21 GPM.

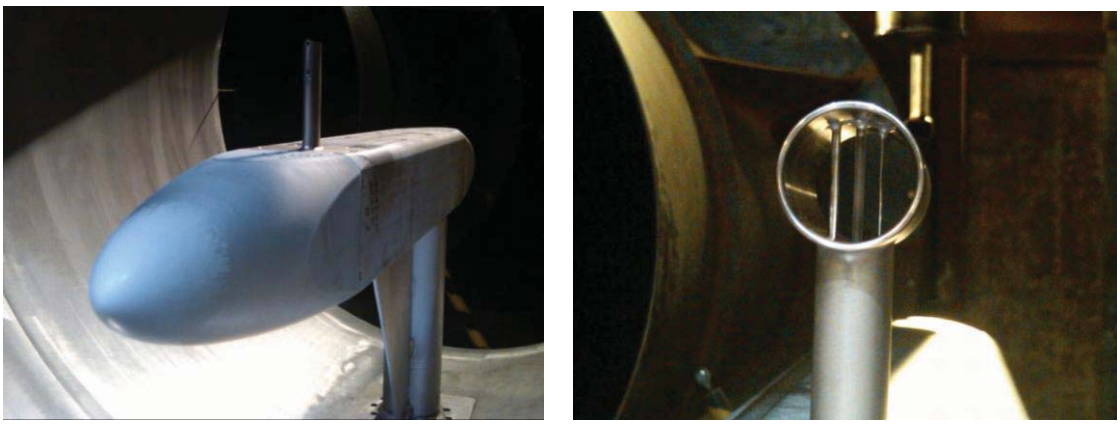

(a) (b)

Figure 9. Water content probes in PSL: (a) robust probe atop the bullet nose mount, (b) multi-wire.

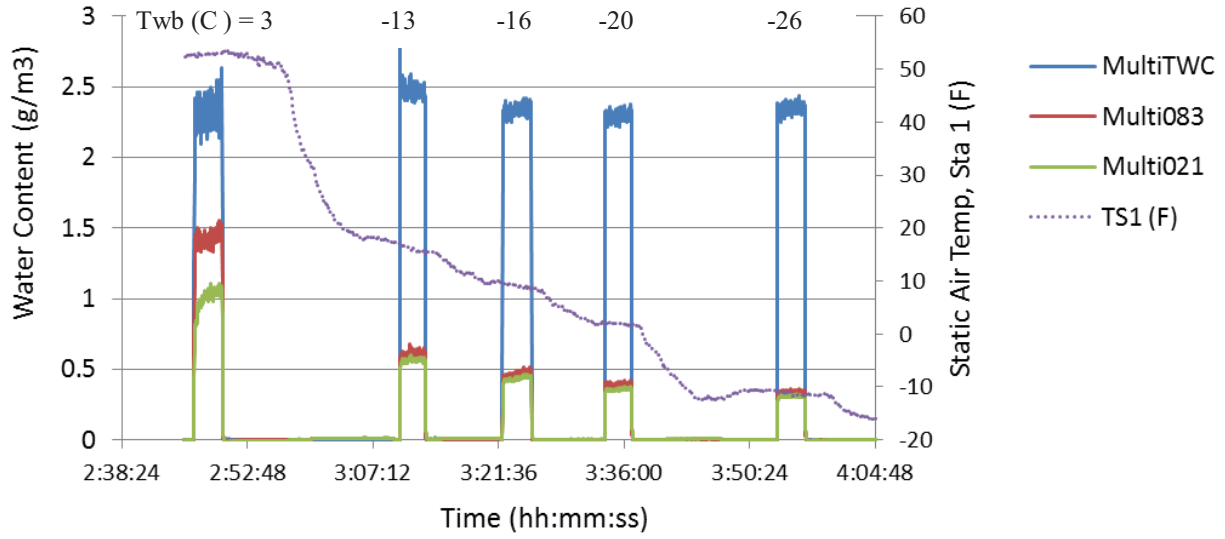

Figure 10. Time trace of multi-wire response as tunnel static air temperature, TS1 (F), cooled toward the target temperature. Altitude, Mach, RH, Pair and DeltaP were held constant. The calculated wet bulb temperature (C) for each spray is indicated above each spray.

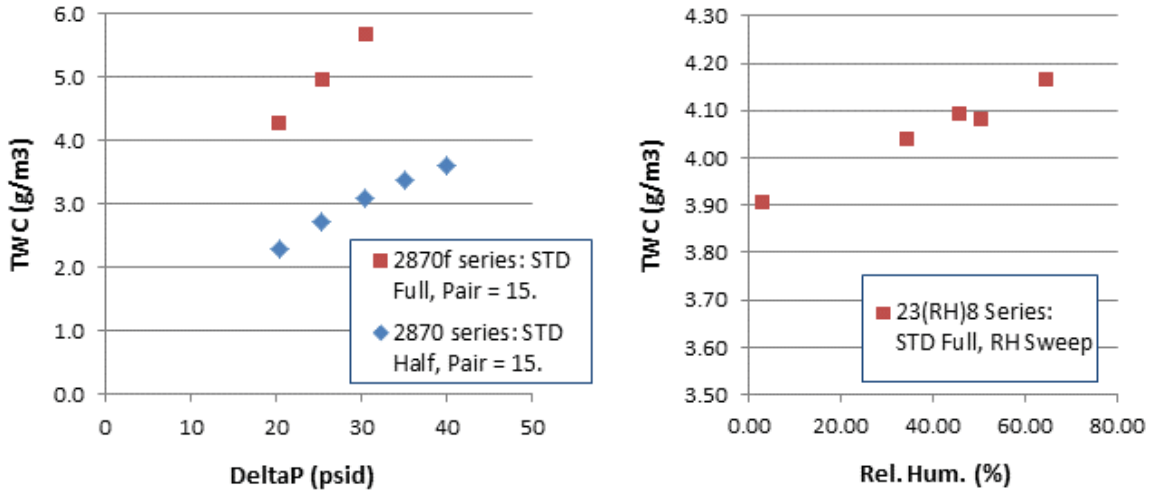

(a) **(b)**

Figure 11. Sample TWC measurements at primary environmental condition. (a) DeltaP sweeps at Pair = 15 psig for Full and Half Standard nozzle patterns, (b) RH sweep where all else was constant.

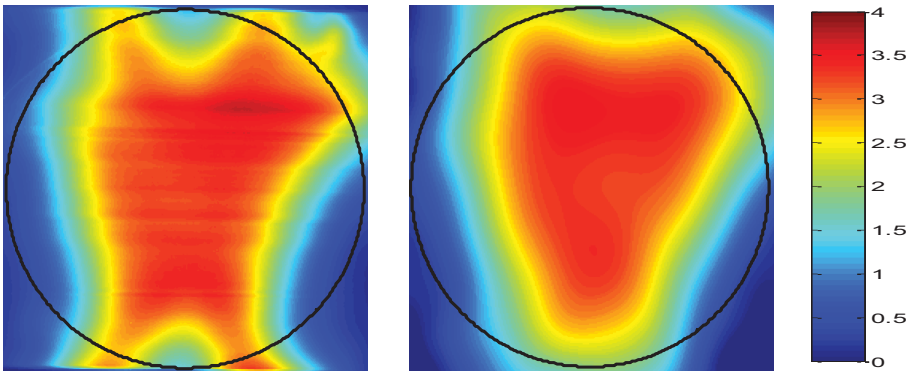

(a) (b)

Figure 12. Comparison of calculated TWC for a given set of conditions from (a) laser sheet for Spray 2523 and (b) tomography for Spray 2923. TWC values for both plots are indicated in g/m^3; the inscribed circle is 24-in.

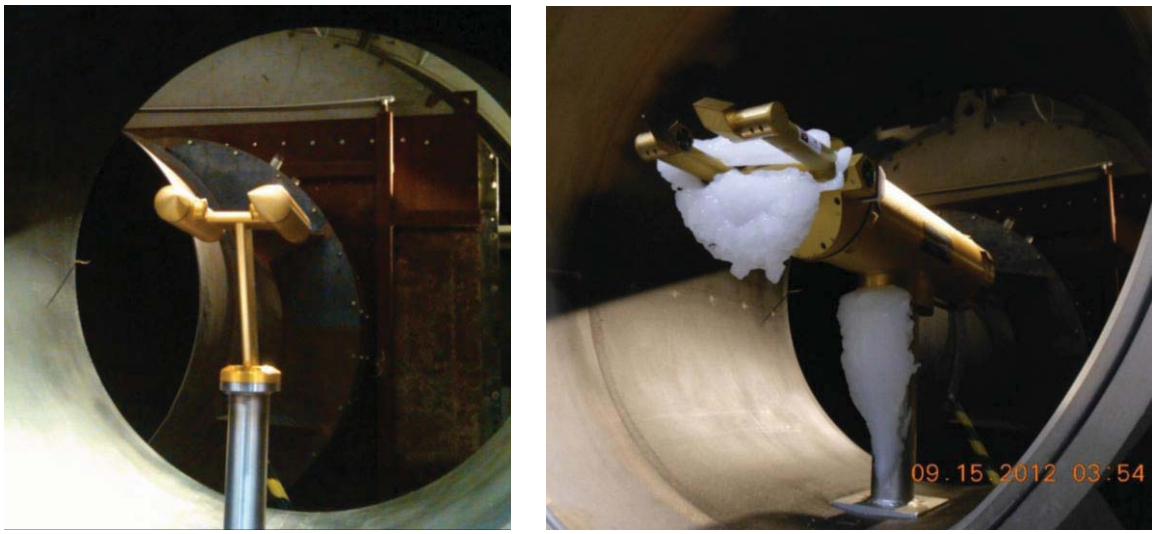

(a) (b)

Figure 13. Particle sizing probes in PSL: (a) CDP, (b) CIP.

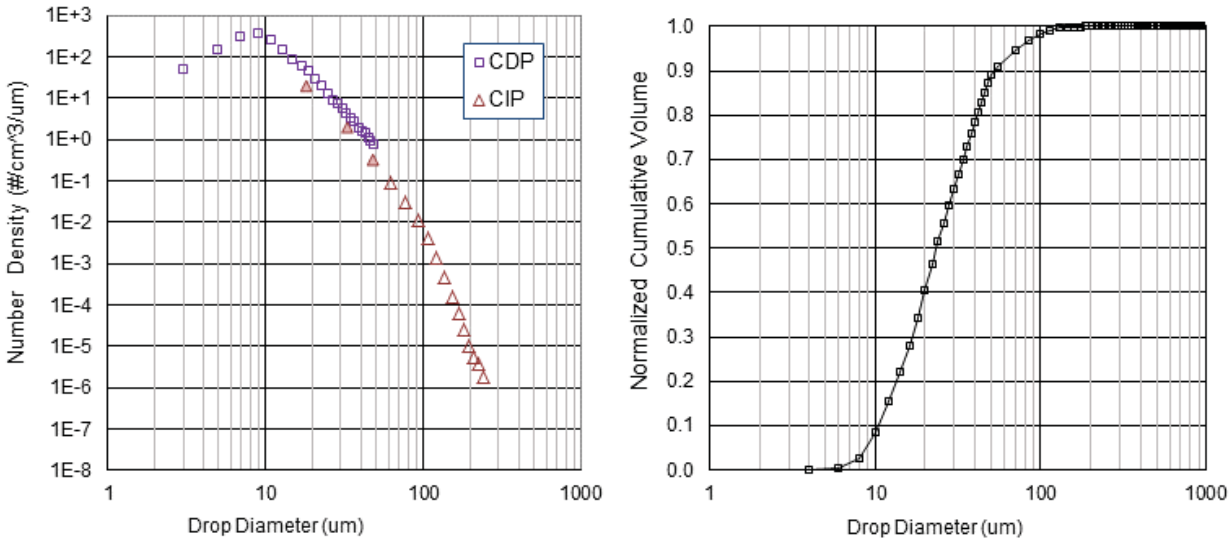

(a) **(b)**

Figure 14. Sample particle size data: (a) size distribution represented by normalized number density from CDP and CIP probes combined and the corresponding (b) normalized cumulative volume distribution. The conditions were the primary altitude and RH, but slower, 120 kts, and warmer, 45F. The spray condition is Standards, Pair = 30 psig, DeltaP = 40 psid.

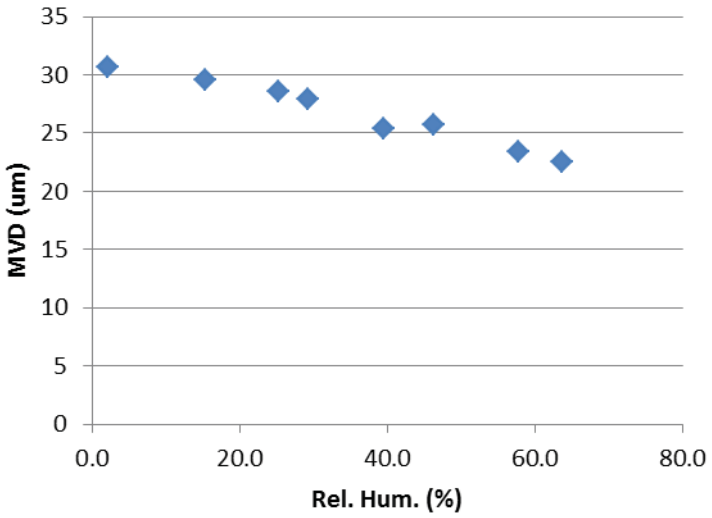

Figure 15. MVD sensitivity to plenum RH at the primay altitude, Pair = 20 psig, DeltaP = 40 psid.